Mon. Not. R. Astron. Soc. **000**, 1–?? (2007) Printed 18 February 2013 (MN LATEX style file v2.2)

The role of minor mergers in the recent star formation history of early-type galaxies

Sugata Kaviraj[1⋆], Sebastien Peirani[1,2], Sadegh Khochfar[1,4], Joseph Silk[1] and Scott Kay[3]

[1] *Department of Physics, University of Oxford, Keble Road, Oxford, OX1 3RH, UK*
[2] *Institut d'Astrophysique de Paris, 98bis, bd Arago - 75014 Paris, France*
[3] *School of Physics and Astronomy, University of Manchester, Oxford Road, Manchester, M13 9PL, UK*
[4] *Max Planck Institut für extraterrestrische Physik, p.o. box 1312, D-85478 Garching, Germany*

18 February 2013

ABSTRACT

We demonstrate that the large scatter in the ultra-violet (UV) colours of intermediate-mass early-type galaxies in the local Universe and the inferred low-level recent star formation in these objects can be reproduced by minor mergers in the standard ΛCDM cosmology. Numerical simulations of mergers with mass ratios ≤ 1:4, with reasonable assumptions for the ages, metallicities and dust properties of the merger progenitors, produce good agreement to the observed UV colours of the early-type population, if the infalling satellites are assumed to have (cold) gas fractions ≥ 20%. Early-types that satisfy $(NUV-r) \lesssim 3.8$ are likely to have experienced mergers with mass ratios between 1:4 and 1:6 within the last ∼ 1.5 Gyrs, while those that satisfy $3.8 < (NUV-r) < 5.5$ are consistent with either recent mergers with mass ratios ≤ 1:6 or mergers with higher mass ratios that occurred more than ∼ 1.5 Gyrs in the past. We demonstrate that the early-type colour-magnitude relations and colour distributions in both the UV and optical spectral ranges are consistent with the expected frequency of minor merging activity in the standard ΛCDM cosmology at low redshift. We present a strong plausibility argument for minor mergers to be the principal mechanism behind the large UV scatter and associated low-level recent star formation observed in early-type galaxies in the nearby Universe.

Key words: galaxies: elliptical and lenticular, cD – galaxies: evolution – galaxies: formation – methods: N-body simulations

1 INTRODUCTION

The formation histories of early-type galaxies remains a controversial and often-debated topic in modern astrophysics. The bulk of the past effort on early-type systems has focussed, almost exclusively, on their *optical* properties. The optical colours of the early-type population are predominantly red, implying that the bulk of the stellar mass in these systems forms at high redshift (e.g. Bower et al. 1992). Furthermore, high α-enhancement ratios in their stellar spectra indicate that this star formation plausibly takes place over short (< 1 Gyr) timescales (e.g. Thomas et al. 1999). However, a drawback of optical data is its lack of sensitivity to moderate amounts of *recent star formation* (RSF), within the last Gyr or so. The optical spectrum remains largely unaffected by the minority of stellar mass that forms in these systems at low and intermediate redshift ($z < 1$), which makes it difficult to measure early-type star formation histories (SFHs) over the last 8 billion years with significant accuracy using optical colours alone.

A first step towards probing early-type SFHs over this period is to quantify their RSF at $z \sim 0$. Rest-frame UV photometry provides an attractive *photometric* indicator of RSF. While its impact on the optical spectrum is relatively weak (and virtually undetectable, given typical observational and theoretical uncertainties), a small mass fraction (< 3%) of young (< 1 Gyr old) stars strongly affects the rest-frame UV spectrum shortward of $3000\mathring{A}$ (Kaviraj 2008). Furthermore, the UV remains largely unaffected by the age-metallicity degeneracy (Worthey 1994) that typically plagues optical analyses (Kaviraj et al. 2007a), making it an ideal photometric indicator of RSF.

In Figure 1 we demonstrate the sensitivity of the UV to small mass fractions of young stellar populations. We construct a model in which an old (10 Gyr old) population contributes 99% of the stellar mass (shown in red), with a

⋆ E-mail: skaviraj@astro.ox.ac.uk

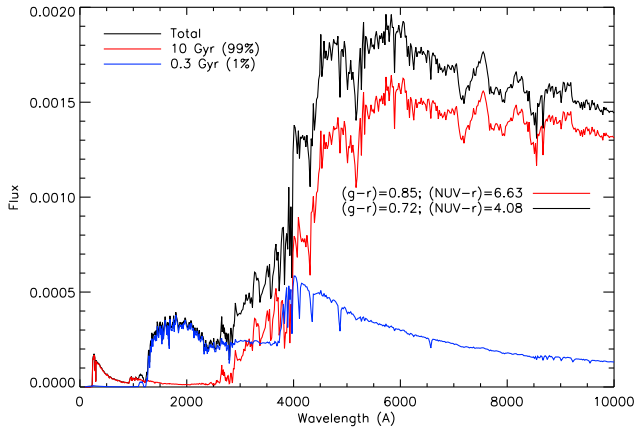

Figure 1. The sensitivity of the UV to small mass fractions of young stellar populations. We construct a model in which an old (10 Gyr old) population contributes 99% of the stellar mass (shown in red), with a 1% contribution from stars that are 0.3 Gyrs old (show in blue). The combined spectral energy distribution (SED) is shown in black. The UV output of the combined SED comes *purely* from the young population (blue) and that the *shape* of the optical spectrum - which determines the optical colours - changes only very slightly. We also indicate the $(g-r)$ and $(NUV-r)$ colours of the combined population (black) with those of the purely old population (red). While the $(g-r)$ colour changes by ~ 0.1 mag from that of a purely old population, the $(NUV-r)$ colour changes by ~ 2.5 mags!

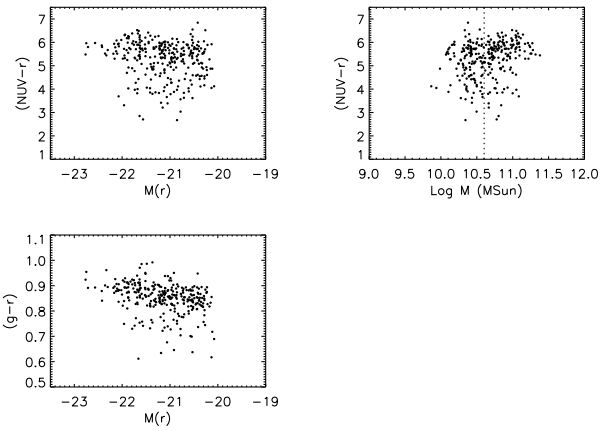

Figure 2. TOP LEFT: The $(NUV-r)$ colour-magnitude relation of nearby $(0.05 < z < 0.06)$ early-type galaxies drawn from the SDSS DR4. Note that the GALEX *NUV* filter is centred at $\sim$ 2300 Å. TOP RIGHT: The $(NUV-r)$ colours of SDSS early-types plotted against their stellar masses, taken from Gallazzi et al. (2005). Note that the Gallazzi et al. masses have been released through the public Garching SDSS catalog which can be found here: http://www.mpa-garching.mpg.de/SDSS/DR4/. The nominal stellar mass adopted for the spheroid in our simulations (4×10^{10} M$_{\odot}$, see Section 2 below) is indicated using the solid line. BOTTOM LEFT: The $(g-r)$ colour-magnitude relation of nearby $(0.05 < z < 0.06)$ early-type galaxies drawn from the SDSS DR4.

1% contribution from stars that are 0.3 Gyrs old (show in blue). The combined spectral energy distribution (SED) is shown in black. The UV output of the combined SED comes *purely* from the young population (blue) and the *shape* of the optical spectrum - which determines the optical colours - changes only very slightly. We also compare the $(g-r)$ and $(NUV-r)$ colours of the combined population (black) and those of the purely old population (red). While the $(g-r)$ colour changes by ~ 0.1 mag from that of a purely old population, the $(NUV-r)$ colour changes by ~ 2.5 mags!

A new generation of early-type studies that have exploited UV data from the GALEX space telescope (Martin et al. 2005) have shown that, in contrast to their optical colour-magnitude relations (CMRs), nearby $(0 < z < 0.11)$, luminous $(M(V) < -21)$ early-types show a large spread in their UV colour distribution of almost 5 mags - a direct consequence of the sensitivity of the UV to small amounts of recent star formation that is demonstrated in Figure 1 above. Following the early work of Yi et al. (2005), Kaviraj et al. (2007b; K07 hereafter) have demonstrated that, while a negligible fraction of the early-type population has photometry consistent with no star formation within the last 2 Gyrs, *at least* 30% show unambiguous signs of RSF, with stellar mass fractions of 1-3% forming within the last Gyr, with luminosity-weighted ages of $\sim 300-500$ Myrs.

In the top left-hand panel of Figure 2 we show the $(NUV-r)$ CMR of nearby $(0.05 < z < 0.06)$ early-type galaxies drawn from the SDSS DR4. Note that the GALEX *NUV* filter is centred at $\sim$ 2300 Å. The large spread in the UV colours is in contrast to the small spread (a few tenths of a mag) in the optical $(g-r)$ colour (bottom left-hand panel). Following K07, early-type morphology is established by visually inspecting each individual object using its SDSS image. The galaxies shown in this figure are selected to have $r < 16.8$, since this is the redshift range within which visual inspection can be robustly performed using SDSS images (see Section 2 in K07). Note that the luminosity of a typical early-type galaxy, in the SDSS r-band, lies around $M(r)^{*} \sim -21.15$ (see Figure 2 in Bernardi et al. 2003). In the right-hand panel of this figure we present the $(NUV-r)$ colours of the SDSS early-types plotted against their *stellar masses*, taken from Gallazzi et al. (2005). Note that the Gallazzi et al. masses have been released through the public Garching SDSS catalog which can be found here: http://www.mpa-garching.mpg.de/SDSS/DR4/. The nominal stellar mass adopted for the spheroid in our simulations is 4×10^{10} M$_{\odot}$ (see also Section 2 below) where the scatter in the UV CMR becomes broad. This value is indicated using a dotted line.

Note that, while the effects of RSF will be present in all diagnostics of star formation (including e.g. the optical $(g-r)$ colour), the sensitivity of a particular indicator depends on the proportional change due to RSF compared to the typical uncertainties in that indicator. These uncertainties come both from measurement errors and from uncertainties in stellar models that are used to convert spectrophotometric quantities (e.g. colours) into estimates of physical parameters such as the ages and mass fractions of young stars. Typical model and observational errors in optical filters are ~ 0.05 mags (Sukyoung Yi priv. comm., see also Yi 2003) and at least 0.02 mags (including calibration uncertainties) respectively. The total resultant uncertainty in the optical $(g-r)$ colours is ~ 0.08 mags (compared to a spread in this colour of ~ 0.3 mags from Figure 2). In a

similar vein, the typical model and theoretical errors in the NUV magnitudes are both around 0.2 mags, yielding uncertainties in the $(NUV - r)$ colours of ~ 0.3 mags (compared to a spread in this colour of almost 5 mags). The enhanced sensitivity of the NUV to RSF stems from the fact that the spread in the NUV colours is significantly (possibly an order of magnitude or more) larger than the uncertainties in the colours. While RSF does leave an imprint on the optical spectrum, the overall sensitivity of the $(NUV - r)$ colour is much greater, making it a much more stringent test of the minor merger hypothesis than can be performed using optical colours alone.

While the UV has revealed the unexpected presence of widespread low-level RSF in the local early-type population, past efforts have only measured the star formation activity without exploring the *physical mechanism* for RSF in these galaxies. In this paper, we explore the potential role of minor mergers in reproducing the UV colour-magnitude relation of intermediate-mass early-type galaxies at $z \sim 0$. It is worth noting that, although low level RSF can produce blue UV colours, only stars formed in the last $\sim$Gyr contribute significantly to the UV flux. Hence, an event like a minor merger - where one expects an *age profile* in the recent star formation - may not automatically produce blue UV colours, even if the supply of cold gas is adequately high to produce the observed mass fraction of young stars. In this study, we combine the results of numerical simulations of minor mergers with standard stellar models to probe the photometric properties of such events and test consistency with the observations, given reasonable assumptions for the properties of the merger progenitors and the predicted frequency of merging activity in the ΛCDM paradigm.

2 SIMULATIONS

In this section we describe the numerical methodology used to study minor mergers between a typical elliptical galaxy and a satellite, where the mass ratio of the system is between 1:4 and 1:10. A more complete description will be provided in Peirani et al. (in prep). Note that the nominal stellar mass of the spheroid used to describe the photometric properties of the simulations in Section 3 matches the region of the $(NUV - r)$ vs. mass plot (see Figure 2 above) where the scatter is broadest.

2.1 Initial conditions

The elliptical is modelled using spherical dark matter (DM) halo and stellar components, with a total mass of $10^{12} M_{\odot}$. Following Jiang & Kochanek (2007), stars contribute 4% of this value. The DM halo follows a Hernquist profile (Hernquist 1990), with parameters chosen so that the inner part coincides with an NFW profile (Navarro et al. 1996) with a virial radius $r_{200} = 206$ kpc and a concentration parameter $C = 10$, as indicated by previous cosmological N-body simulations (Dolag et al. 2004). A Hernquist profile reproduces the 'de Vaucouleurs' $R^{1/4}$ surface brightness profiles of typical elliptical galaxies. The effective radius of the projected brightness is $r_e = 4.3$ kpc.

The satellite is constructed using a spherical DM halo (with a Hernquist profile) which contains a disk containing stars and gas but no bulge. The mass of the disk represents 5% of the total mass, with a gas fraction of either 20% or 40%. The gas fractions are consistent with the observed values from the SDSS (Kannappan 2004). Satellites are created following Springel et al. (2005) and their rotation curves satisfy the baryonic Tully-Fisher relation. In all simulations satellites are put on prograde parabolic orbits (Khochfar & Burkert 2006), with a pericentric distance $R_p = 8$ kpc, and initial separations of 100 kpc.

2.2 Numerical method

The simulations are performed using the public GADGET2 code (Springel 2005) with added prescriptions for cooling, star formation and feedback from Type Ia and II supernovae (SN). Approximately 380,000 particles are used for each experiment and the particle masses and gravitational softening lengths (ϵ) involved are summarized in the table below.

	DM	gas	star (disk)	star (E)
Mass ($10^5 M_{\odot}$)	30.3	4.5	4.5	13.5
ϵ (kpc)	0.4	0.5	0.5	0.4

The cooling and star formation (SF) recipes follow the prescriptions of Thomas & Couchman (1992) and Katz et al. (1996) respectively. Gas particles with $T > 10^4$K cool at constant density (with the assumption of solar metallicity) for the duration of each timestep. Gas particles with $T < 2 \times 10^4 K$, number density $n > 0.1\, cm^{-3}$, overdensity $\delta\rho_{gas} > 100$ and $\nabla.\upsilon < 0$ form stars according to the standard star formation prescription: $d\rho_*/dt = c_* \rho_{gas}/t_{dyn}$, where ρ_* refers to the stellar density, t_{dyn} is the dynamical timescale of the gas and c_* is the SF efficiency. Instead of creating new (lighter) star particles, we implement the SF prescription in a probabilistic fashion. Assuming a constant dynamical time across the timestep, the fractional change in stellar density, $\Delta\rho_*/\rho_* = 1 - \exp(-c_* \Delta t/t_{\rm dyn})$. For each gas particle, we draw a random number (r) between 0 and 1 and convert it to a star if $r < \Delta\rho_*/\rho_*$.

The energy injection into the inter-stellar medium (ISM) from SN, which regulates the star formation rate (SFR), is modelled following the approach of Durier & de Freitas Pacheco (2007, in prep.). Instead of assuming 'instantaneous' energy injection, we include the effective lifetime of SN progenitors using the rate of energy injection H_{SN}. For this, we consider stellar lifetimes in the mass ranges $0.8\, M_{\odot} < m < 8.0\, M_{\odot}$ and $8.0\, M_{\odot} < m < 80.0\, M_{\odot}$ for Type Ia and Type II progenitors respectively. Using a Salpeter initial mass function for Type II SN gives:

$$H_{SN_{II}} = 2.5 \times 10^{-18} \Big(\frac{m_*}{M_{\odot}}\Big) E_{SN} \Big(\frac{1300}{\tau(\mathrm{Myr}) - 3}\Big)^{0.24} \mathrm{erg.s}^{-1} \quad (1)$$

where $E_{SN} = 10^{51}$ erg, m_* is the mass of the star particle and $3.53 < \tau < 29$ Myr. For Type Ia SN, the heating is delayed, since they appear $t_0 = 0.8 - 1.0$ Gyr after the onset of star formation. Following de Freitas Pacheco (1998), the probability of one event in a timescale τ after the onset of star formation is given by:

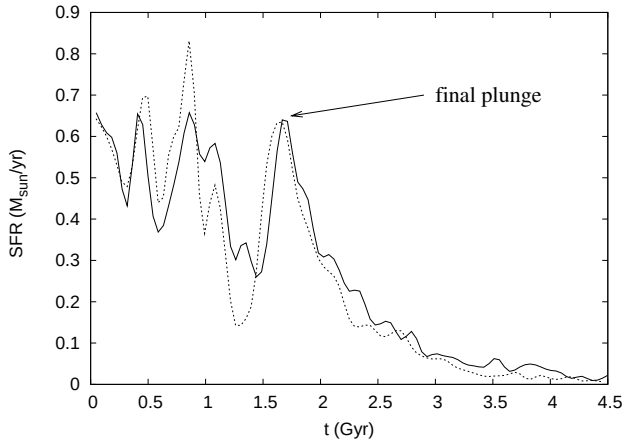

Figure 3. The star formation rate of a minor major with mass ratio 1:6, where the gas fraction of the satellite is 20% and $c_* = 0.05$. The dashed line represents the same simulation with 10 times more particles. At the 'final plunge' the satellite disappears into the parent elliptical, so that images (e.g. through an SDSS r-band filter) would indicate a single spheroidal object.

$$H_{SN_{I_a}} = 4.8 \times 10^{-20} \Big(\frac{m_*}{M_\odot}\Big) E_{SN} \Big(\frac{t_0}{\tau}\Big)^{3/2} \mathrm{erg.s}^{-1} \qquad (2)$$

Eqns (1) and (2) are used to compute the energy released (E_i) by SN derived from a star particle i, and a fraction γ of this energy is deposited in the jth neighbour gas particle by applying a radial kick to its velocity with a magnitude $\Delta v_j = \sqrt{(2 w_j \gamma E_i / m_j)}$, where w_j is the weighting based on the smoothing kernel and m_j is the mass of gas particle j. We note that all gas neighbours are located in a sphere of radius R_{SN}, centered on the SN progenitor, to avoid spurious injection of energy outside the SN's region of influence.

In the simulations presented in this study, we use $\gamma = 0.1$, $R_{SN} = 0.4$ kpc and vary c_* in the range $0.01 < c_* < 0.1$. When satellites are isolated, these parameters lead to a quasi-constant SFR between 0.2 and 3.0 $M_\odot \mathrm{yr}^{-1}$, depending on the mass and initial gas fraction of the satellite. These SFRs are in good agreement with those for low-mass objects found in previous simulations of isolated galaxies (e.g. Stinson et al. 2006).

Finally, we have checked that increasing the resolution of the simulations (by a factor of 10) does not affect the star formation history or the derived colours so that the conclusions presented in this work are robust. A typical example of the SFH is shown in Figure 3.

3 THE CASE FOR MINOR MERGERS

We begin by exploring the predicted photometry from an ensemble of minor merger simulations (described in Section 2) with the assumptions that (a) both merger progenitors have solar metallicity, (b) the elliptical and satellite have luminosity-weighted ages of 9 and 5 Gyrs respectively and (c) the dust extinction due to the ISM in the remnant is given by $E^{ISM}_{B-V} \sim 0.05$.

We briefly describe the motivation for modelling the underlying population of the spheroid using a 9 Gyr old simple stellar population (SSP). It is well established that the bulk of the stellar populations in elliptical galaxies are uniformly old. This is demonstrated by the fact that (a) they show red optical colours with small scatter (e.g. Bower et al. 1992; Stanford et al. 1998) and (b) they exhibit high alpha-enhancement (e.g. [Mg/Fe]) ratios, which implies that the star formation took place on timescales shorter than the typical onset timescales of Type Ia supernovae i.e. < 1 Gyrs (see e.g. Thomas et al. 1999). Hence the underlying population can be approximated by an old SSP. The particular choice of 9 Gyrs is motivated by the fact that Bernardi et al. (2003), who recently studied the SDSS elliptical galaxy population in the nearby Universe, were able to fit their optical colour-magnitude relations with an SSP with an age of 9 Gyrs. It is worth noting that *optical* colour evolution virtually stops after ~ 6 Gyrs (Yi 2003). This means that a 6 Gyr old SSP looks very similar to an older stellar population e.g. 9 Gyrs. In other words we could replace the 9 Gyr SSP with a 6 or 10 Gyr SSP and our results will not change. Note that similar techniques (i.e. using an old SSP to represent the underlying stellar population of ellipticals) have been frequently used by previous studies. e.g. Trager et al. (2000) and Ferreras & Silk (2000). Finally, stellar populations that are older than ~ 2 Gyrs do not contribute to the UV (see the bottom panel of Figure 7 in K07). As a result, the *underlying* population of an elliptical galaxy will not contribute to the UV at all.

The estimate for the ISM extinction is an average value for local early-types, derived by K07 from parameter estimation using GALEX (UV) and SDSS (optical) photometry. Since the youngest stars are expected to reside in molecular clouds (MCs) which have short lifetimes of a few tens of Myrs (e.g Blitz & Shu 1980; Hartmann et al. 2001) and dust extinction several times larger than that due to the ISM alone (e.g. Charlot & Fall 2000), we explore MC lifetimes in the range 0-50 Myrs and MC extinctions in the range $0.05 < E^{MC}_{B-V} < 0.5$. Thus, when the synthetic photometry from the simulations is constructed, stars with ages less than the MC lifetime in question are subject to the prescribed MC extinction. The stellar models used in this study are described in Yi (2003).

In Figure 4 we present the synthetic photometry from various configurations for mergers with mass ratios of 1:10. The remnant is 'observed' at the point where the satellite finally disappears into the parent elliptical, so that images (e.g. through an SDSS r-band filter) would indicate a single spheroidal object. The colours shown are therefore the *bluest* possible for each scenario where the system appears to be one object. Star formation declines after this 'final plunge' (see Figure 3) and the remnant reddens, in the $(NUV - r)$ colour, by ~ 0.8 mag/Gyr for mass ratios of 1:4 and 1:6 and by ~ 0.5 mag/Gyr for a mass ratio of 1:10.

We find that, with reasonable MC properties - e.g. lifetimes ≥ 30 Myrs (red and green colours) and high dust extinctions (large symbols) - 1:10 mergers can reproduce most but not all of the scatter in the observed UV colours. In particular, the *bluest* UV colours ($NUV - r \lesssim 4$) cannot be accounted for by 1:10 mergers because the RSF induced is inadequate, even when the satellite has a high gas fraction ($\sim 40\%$). The observed early-type UV colour-magnitude relation (CMR; shown using filled grey circles in Figure 4) is restricted to the redshift range $0.05 < z < 0.06$ (to ensure

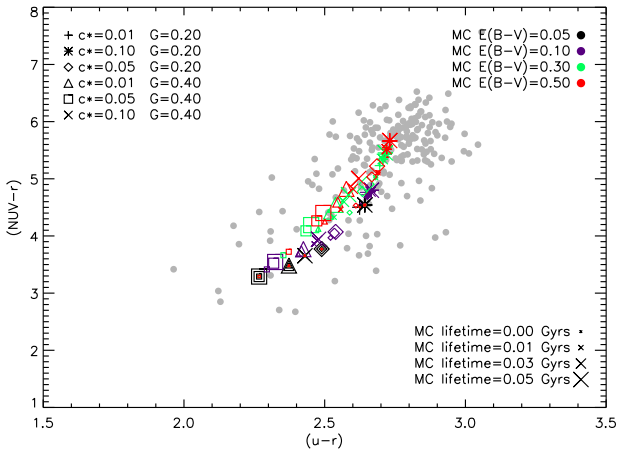

Figure 4. Predicted photometry from an ensemble of minor merger simulations with mass ratios of 1:10. Both progenitors are assumed to have solar metallicity with the elliptical and the satellite having ages of 9 and 5 Gyrs respectively. The ISM dust extinction in the remnant is given by $E^{ISM}_{B-V} \sim 0.05$. Symbol types represent merger configurations - the star formation efficiency ($c*$) and gas fraction (G) of the accreted satellites are shown in the top left legend. MC extinctions are shown using colours, while symbol sizes represent MC lifetimes. Grey dots represent the observed colours of luminous (L^* or above) early-type galaxies in the redshift range $0.05 < z < 0.06$. Note that typical uncertainties in the observed colours are 0.2 mag and that the synthetic photometry has been redshifted to $z = 0.065$ for a direct comparison.

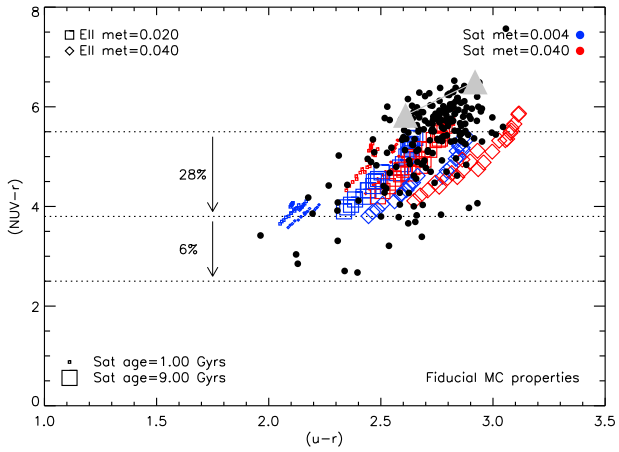

Figure 5. TOP: Predicted photometry from an ensemble of minor mergers with mass ratios of 1:10. We assume a spread in the age (1-9 Gyrs; shown using symbol sizes) and metallicity ($0.2Z_\odot - 2Z_\odot$; shown using colours) of the satellite. The observed colours of the local, intermediate-mass (L^* or above) early-type population is shown by the black dots. Large grey triangles indicate the positions of simple stellar populations with half-solar and solar metallicities that form at $z = 3$.

robust morphological classification from SDSS images) and $r < 16.2$ (which corresponds to galaxies more luminous than L^* at this redshift).

Recalling that Figure 4 assumes solar metallicity and a single age for the satellite (5 Gyrs), we now explore a wider parameter space where we vary the metallicity of the satellite in the range $0.2Z_\odot$ to $2Z_\odot$ and its luminosity-weighted age in the range 1-9 Gyrs. The analysis is restricted to realistic MC properties - lifetimes $\gtrsim$ 30 Myrs and extinction $\gtrsim$ 0.3. We present these results in Figure 5. While the predicted photometry falls in the centre of the locus of observed galaxies in Figure 4, we find that a reasonable spread in the age and metallicity of the satellite can reproduce the 'horizontal' spread in the $(u-r)$ colours. However, such a spread in age and metallicity cannot mimic low MC lifetimes/extinctions i.e. if we restrict our analysis to realistic MC properties only, low satellite ages and metallicities remain unable to reproduce the bluest UV colours. We also indicate, in Figure 5, the early-type galaxy fractions bluer than $(NUV - r) < 3.8$ (the colour limit of the 1:10 mergers with realistic MC properties) and in the colour range $3.8 < NUV - r \leq 5.5$. K07 estimated that, within theoretical and observational uncertainties, galaxies bluer than $(NUV - r) \sim 5.5$ are very likely to have had some RSF (within the last ∼Gyr), while galaxies with $(NUV - r) \geq 5.5$ can be consistent with both RSF and purely old (> 2 Gyrs old) stellar populations.

We now repeat the analysis with mergers that have mass ratios of 1:6 and 1:4. Figure 6 indicates that the blue end of the early-type UV colours, which is inconsistent with 1:10 mergers, can indeed be reproduced by 1:6 and 1:4 mergers with realistic assumptions for MC properties.

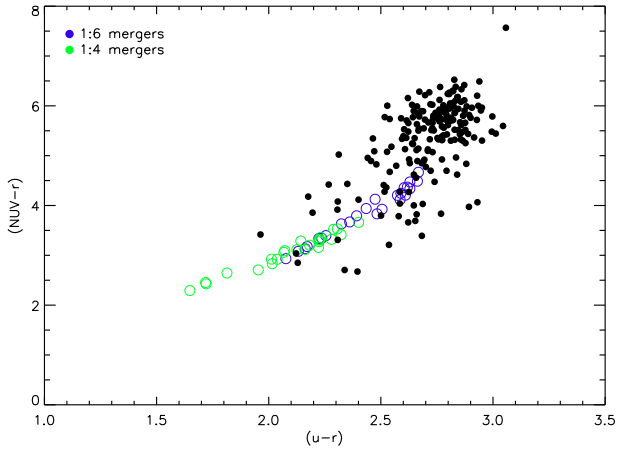

Figure 6. Predicted photometry from the same ensemble of minor merger simulations as in Figure 4 but with mass ratios of 1:6 (blue) and 1:4 (red). Both progenitors are assumed to have solar metallicity with the elliptical and the satellite having ages of 9 and 5 Gyrs respectively. The ISM dust extinction in the remnant is given by $E^{ISM}_{B-V} \sim 0.05$. We only show configurations with realistic MC properties - lifetimes $\gtrsim$ 30 Myrs and extinction $\gtrsim$ 0.3

4 MERGER STATISTICS IN ΛCDM AND REPRODUCTION OF THE OBSERVED EARLY-TYPE COLOURS

While the UV colours of intermediate-mass early-type galaxies appear consistent with minor mergers, the reproducibility of the entire UV CMR depends on the frequency of merging activity at low redshift. In Figure 7 we present the average fraction of early-type galaxies (in dark matter halos of mass 10^{12} $M_{\odot}$ or above) that are predicted to have had one (solid), two (dashed), three (dot-dashed) and four (triple dotted) 1:X mergers in a given look-back time in ΛCDM. The value of 'X' is indicated in each panel. Merger trees are generated using the semi-analytical model of Khochfar and Burkert (2003, 2005) and Khochfar & Silk (2006) and morphology is traced using stellar bulge:total (B/T) ratios - early-type galaxies are assumed to have $B/T > 0.7$.

The merger fractions are calculated by dividing the number of mergers that occurred in look-back time (t) bins in the histories of spheroids by the number of such spheroids at $z = 0$. For example, the point at $t = 0$ represents the merger fraction within look-back times of 0 and 1 Gyr, while the point at $t = 1$ represents the merger fraction within look back times of 1 and 2 Gyrs and so on. The merger fraction increases with look-back time because the merger rate in the Universe increases at higher redshift (see also e.g. Gottlöber et al. 2001; Le Fèvre et al. 2000). Note that the merger fraction increases monotonically until the merger rate in the Universe peaks and then drops off.

Before comparing the photometric predictions from our model machinery to the observations, we briefly note that, while major mergers (which have mass ratios between 1:1 and 1:3) might also be expected to contribute to the scatter in the UV CMR, a study of the GALEX *NUV* photometry of a sample of *ongoing* major mergers, identified by McIntosh et al. (2007) from the SDSS, indicates that major merger progenitors lie on the broad UV red sequence ($NUV - r > 4.7$). While a caveat here is that the McIntosh et al. sample is small (compared to the SDSS galaxy population and especially after cross-matching with GALEX), it is reasonable to conclude that major mergers will contribute only to the broadness of UV 'red sequence' ($NUV - r > 4.7$), not to the full extent of the UV scatter and certainly not to the blue end of the UV CMR.

We now check if the predicted LCDM minor merger activity (i.e. events with mass ratios between 1:4 and 1:10), convolved with the predictions from the basic set of numerical simulations described above, is able to simultaneously reproduce the UV and optical CMRs of the low-redshift early-type population. Using the SDSS luminosity function of low-redshift early-type galaxies extracted in K07, we construct a large Monte-Carlo (MC) ensemble of 50,000 simulated objects and compare the synthetic CMRs from this ensemble with the observed early-type CMRs in both the ($NUV - r$) and ($g - r$) colours. We assume (a) realistic MC properties i.e. random MC lifetimes between 30 and 50 Myrs and $0.3 < E^{MC}_{B-V} < 0.5$ (b) a gaussian distribution in the SSP-weighted satellite ages, which peaks at 5 Gyrs, with a width of 2 Gyrs and (c) a uniform distribution in the satellite metallicities in the range $0.2Z_{\odot} - 2Z_{\odot}$. We only consider merger events within the last 2.5 Gyrs and note that including larger time windows does not alter our results because the UV flux decays rapidly after 2 Gyrs anyway.

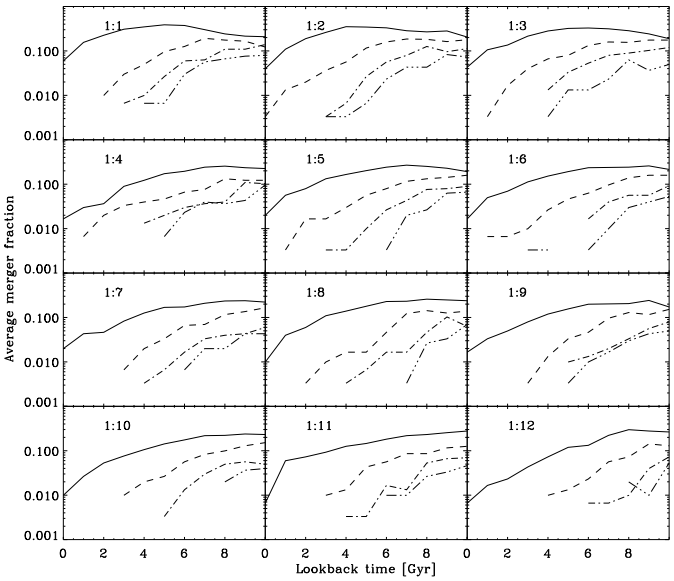

Figure 7. The average fraction of spheroidal galaxies (in dark matter halos of mass 10^{12} $M_{\odot}$ or above) that are predicted to have had one (solid), two (dashed), three (dot-dashed) and four (triple dotted) 1:X mergers in a given look-back time in ΛCDM. The value of 'X' is indicated in each panel and the dispersions in the fractions are $\sim 20\%$. Fractions are calculated by dividing the number of mergers that occurred in look-back time (t) bins in the histories of spheroids by the number of such spheroids at $z = 0$. For example, the point at $t = 0$ represents the merger fraction within a look-back time of 0 and 1 Gyr, while the point at $t = 1$ represents the merger fraction within a look back time of 1 and 2 Gyrs and so on. The merger fraction increases with look-back time because the merger rate in the Universe increases at higher redshift (see also e.g. Gottlöber et al. 2001; Le Fèvre et al. 2000). Note that the merger fraction increases monotonically until the merger rate in the Universe peaks and then drops off.

In Figure 8 we draw a random subset, equal to the number of observed galaxies in our comparison redshift range ($0.05 < z < 0.06$), from the parent MC ensemble of 50,000 objects and compare their ($NUV - r$) and ($g - r$) colours to that of the observed early-type population. A comparison between the colour histograms of the parent MC ensemble and the observed early-type population is also shown in the inset to each figure. Note that both histograms are normalised to 1. We find that, given the assumptions listed above, there is good quantitative agreement between the synthetic and observed CMRs and colour distributions in both UV and optical colours. In other words, the predicted minor merger activity in the standard model is able to reproduce the UV/optical properties of the early-type population (in particular the distribution scatter to blue UV colours) with a satisfactory level of accuracy. This, in turn, provides a very strong plausibility argument for minor merging driving the recent star formation observed in early-type galaxies at low redshift.

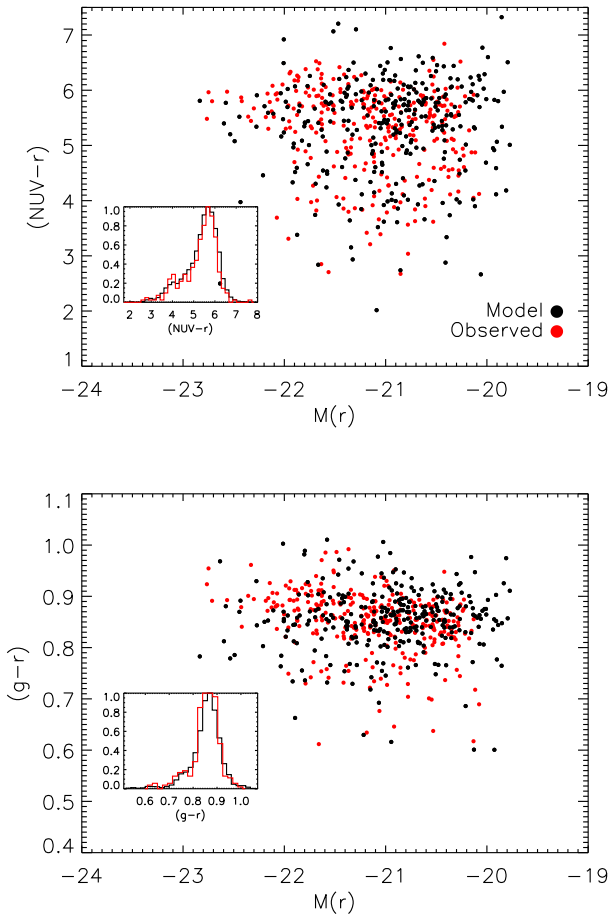

Figure 8. TOP: Comparison of the simulated $(NUV-r)$ colours, generated by convolving the photometric predictions from minor merger simulations with the predicted minor merger activity in LCDM (black), with the observed $(NUV-r)$ colours of the low-redshift early-type population. Colour histograms (normalised to 1) are shown in the inset. BOTTOM: The corresponding plot for the optical $(g-r)$ colour.

4.1 A note about observational signatures of merging

It is worth noting here that the arguments presented above imply that an appreciable number of early-type systems in the nearby Universe should either be in a 'closepair' or 'pre-merger' system with a satellite or exhibit morphologies that are consistent with recent merging events.

We should mention first that several observational studies have looked at closepairs from a variety of surveys across a range of redshifts (e.g. Patton et al. 2000; Le Fèvre et al. 2000). While such studies are very useful, a potential complication is that the detection of closepairs relies on a range of criteria. Patton et al. (2000), for example, tag pairs of galaxies as 'pre-mergers' where the tranverse separation on the sky is less than $20h^{-1}$ kpc and the relative velocities are less than 500 kms^{-1}. The number of closepairs naturally depends on the criteria being used. For example, making the criteria stricter increases the likelihood that each candidate system is truly a 'pre-merger'. However it also results in fewer pre-mergers being found in total. An added problem is that computing relative velocities requires spectroscopic redshifts. As a result smaller, fainter galaxies at the magnitude limit of typical spectroscopic surveys will not have redshifts and therefore minor mergers cannot be efficiently identified (since only the larger progenitor has a redshift). Hence the lack of large numbers of minor merger closepairs in typical observational studies is not a good indicator of the true frequency of such events in the nearby Universe.

A better alternative is to look for *post-mergers* i.e. objects that show tell-tale signatures of recent merger activity. An added advantage of studying post-merger systems is that one is sure that the merger has actually taken place, whereas with pre-merger systems it is just a guess (albeit a well-educated one!). While a large observational survey like the SDSS could be the perfect test-bed for performing such a study, the typical 50 second exposure SDSS images are not deep enough to detect faint morphological disturbances from minor mergers. However, van Dokkum (2005) have recently used very deep optical photometry to show that over 70% of early-types on the optical *red* sequence show morphological signatures of merging. The morphological features, e.g. fans, tails, shells, are faint and red to surface brightness limits of $\mu \sim 28$ mag arcsec^{-2}) and consistent with minor mergers (where the induced star formation is at a very low-level). These features do not appear in the corresponding SDSS images and an analysis of the UV magnitudes of these red mergers (using GALEX) indicates that their UV CMR is similarly broad to what has been found for the general SDSS early-type population in K07 (Kaviraj and van Dokkum, in prep).

5 DISCUSSION AND SUMMARY

We have compared the UV colours of nearby ($0.05 < z < 0.06$) early-type galaxies with synthetic photometry derived from numerical simulations of minor mergers, with reasonable assumptions for the ages, metallicities and dust properties of the merger progenitors. *Observational* estimates for satellite gas fractions have been taken from Kannappan (2004) and minor merger simulations have been performed using these gas fractions. We have then appealed to the merger statistics in the standard ΛCDM paradigm to check whether the minor merger activity could plausibly drive the scatter in the UV CMR at low redshift.

We have found that the bluest end of the early-type UV CMR ($NUV - r < 3.8$) is consistent with mergers that have mass ratios between 1:4 and 1:6 (and cannot be reproduced by events with mass ratios less than or equal to 1:10), assuming that the infalling satellites have gas fractions around $\sim$ 20% or higher, which are consistent with the observationally constrained gas fractions from Kannappan (2004). Early-types with intermediate UV colours ($3.8 < NUV-r < 5.5$) are consistent with either recent minor mergers with mass ratios less than 1:6 or mergers with higher mass ratios more than $\sim$ 1 Gyr in the past. Major mergers are likely only to contribute to the broadness of the UV red sequence and not to the blue scatter in the UV CMR. Furthermore, we have demonstrated that the predicted minor merger activity in the standard model, convolved with photometric predictions from our fiducial set of numerical simulations, is

able to simultaneously reproduce the UV and optical CMRs and colour distributions of the low-redshift early-type population, in particular the large scatter to blue colours. This, in turn, provides a strong plausibility argument for minor mergers being responsible for the RSF in early-type galaxies in the nearby Universe.

We note here that our study does not utilise a full-blown semi-analytical model for two important reasons. Firstly, the amount of gas available at late times in such a model depends on the baryonic recipes implemented within it. Different models can predict different gas fractions in satellites at late times. Secondly, in current semi-analytical models the merger event is modelled 'instantaneously' i.e. the full age profile of stars formed in the merger is not taken into account. The correct way to implement minor merger events in a semi-analytical model is to apply star formation histories from simulations such as those presented in this paper to merger events in the model. A full analysis with such an implementation will be provided in a forthcoming paper (Khochfar et al., in prep). In this paper we have appealed *only* to the merger fractions predicted by LCDM, which are robust. Finally, the primary reason for using the Khochfar and Burkert model is that it uses the Extended Press Schechter (EPS) formalism to generate merger trees, resulting in infinite mass resolution which is important because we are specifically looking at minor mergers involving small (satellite) objects.

Finally, we note some possible caveats to the analysis presented here. Firstly, although it is reasonable to infer relatively high gas fractions ($> 20\%$) for infalling satellites based Kannappan (2004), it is worth noting that the gas fractions are derived from calibrations calculated by combining SDSS photometry and HI measurements. Confirmation of these gas fractions (especially in satellite galaxies) requires larger and deeper surveys that yield gas mass measurements, which are unavailable right now but may be possible using future instruments such as Herschel. Secondly, we note that although cooling from hot gas halos could potentially contribute to the supply of cold gas that then drives star formation, this channel is unlikely in galaxies in the mass range studied here. Dekel & Birnboim (2006) show that, at late epochs ($z < 2$), the gas in halos above a critical shock-heating mass ($10^{12}\mathrm{M}_{\odot}$; consistent with the galaxies considered in this study) is heated by a virial shock, leading to long cooling timescales that effectively shut down the gas supply and subsequent star formation. Furthermore, unchecked accretion from hot gas halos would result in early-types becoming too massive and too blue (Benson et al. 2003). Since there is no reason to believe that that $z \sim 0$ is a preferential epoch for gas cooling, evidence from the luminosity function of massive galaxies renders star formation from cooling flows very unlikely. This, combined with the abundance of minor merger features in the van Dokkum (2005) study, strongly indicates that the recent star formation is driven not by gas cooling but by merging activity.

While this study provides a strong plausibility argument for minor mergers being the principal mechanism behind the large UV scatter and associated low-level recent star formation in early-type galaxies, similar studies are required at intermediate redshifts ($0.5 < z < 1$) to check whether the evolution of this scatter is consistent with the ΛCDM merger statistics. In addition, deep/high-resolution imaging i.e. with the Hubble Space Telescope are required to confirm the *coincidence* of morphological signatures produced by merging with UV excess in these galaxies. Current galaxy surveys such as COSMOS (Scoville et al. 2007) make such analyses possible and results from such studies will be presented in a forthcoming paper.

ACKNOWLEDGEMENTS

We warmly thank the anonymous referee for an insightful review that considerably improved the quality of the original manuscript. Sugata Kaviraj acknowledges a Leverhulme Early-Career Fellowship (till Oct 2008), a Research Fellowship from the Royal Commission for the Exhibition of 1851 (from Oct 2008), a Beecroft Fellowship from the BIPAC Institute and a Senior Research Fellowship from Worcester College, Oxford. S. Peirani acknowledges support from ANR. Finally, we thank J. A. de Freitas Pacheco, F. Durier, I Ferreras, S. K. Yi and A. Pipino for stimulating conversations.

REFERENCES

Benson A. J., Bower R. G., Frenk C. S., Lacey C. G., Baugh C. M., Cole S., 2003, ApJ, 599, 38
Bernardi M., collaboration S., 2003, AJ, 125, 1849
Blitz L., Shu F. H., 1980, ApJ, 238, 148
Bower R. G., Lucey J. R., Ellis R., 1992, MNRAS, 254, 589
Charlot S., Fall S. M., 2000, ApJ, 539, 718
de Freitas Pacheco J. A., 1998, AJ, 116, 1701
Dekel A., Birnboim Y., 2006, MNRAS, 368, 2
Dolag K., Bartelmann M., Perrotta F., Baccigalupi C., Moscardini L., Meneghetti M., Tormen G., 2004, A&A, 416, 853
Ferreras I., Silk J., 2000, ApJL, 541, L37
Gallazzi A., Charlot S., Brinchmann J., White S. D. M., Tremonti C. A., 2005, MNRAS, 362, 41
Gottlöber S., Klypin A., Kravtsov A. V., 2001, ApJ, 546, 223
Hartmann L., Ballesteros-Paredes J., Bergin E. A., 2001, ApJ, pp 852–868
Hernquist L., 1990, ApJ, 356, 359
Jiang G., Kochanek C. S., 2007, ArXiv:0705.3647, 705
Kannappan S. J., 2004, ApJ, 611, L89
Katz N., Weinberg D. H., Hernquist L., 1996, ApJS, 105, 19
Kaviraj S., 2008, ArXiv:0710.1311, 710
Kaviraj S., GALEX collaboration 2007b, ApJS, 173, 619
Kaviraj S., Rey S.-C., Rich R. M., Yoon S.-J., Yi S. K., 2007a, MNRAS, 381, L74
Khochfar S., Burkert A., 2003, ApJ, 597, L117
Khochfar S., Burkert A., 2005, MNRAS, 359, 1379
Khochfar S., Burkert A., 2006, A&A, 445, 403
Khochfar S., Silk J., 2006, MNRAS, 370, 902
Le Fèvre O., Abraham R., Lilly S. J., Ellis R. S., Brinchmann J., Schade D., Tresse L., Colless M., Crampton D., Glazebrook K., Hammer F., Broadhurst T., 2000, MNRAS, 311, 565
Martin D. C., GALEX collaboration 2005, ApJ, 619, L1

McIntosh D. H., Guo Y., Hertzberg J., Katz N., Mo H. J., van den Bosch F. C., Yang X., 2007, ArXiv e-prints, 710
Navarro J. F., Frenk C. S., White S. D. M., 1996, ApJ, 462, 563
Patton D. R., Carlberg R. G., Marzke R. O., Pritchet C. J., da Costa L. N., Pellegrini P. S., 2000, ApJ, 536, 153
Scoville N., COSMOS collaboration 2007, ApJS, 172, 1
Springel V., 2005, MNRAS, 364, 1105
Springel V., Di Matteo T., Hernquist L., 2005, MNRAS, 361, 776
Stanford S. A., Eisenhardt P. R. M., Dickinson M., 1998, ApJ, 492, 461
Stinson G., Seth A., Katz N., Wadsley J., Governato F., Quinn T., 2006, MNRAS, 373, 1074
Thomas D., Greggio L., Bender R., 1999, MNRAS, 302, 537
Thomas P. A., Couchman H. M. P., 1992, MNRAS, 257, 11
Trager S. C., Faber S. M., Worthey G., González J. J., 2000, AJ, 120, 165
van Dokkum P. G., 2005, AJ, 130, 2647
Worthey G., 1994, ApJS, 95, 107
Yi S. K., 2003, ApJ, 582, 202
Yi S. K., Yoon S.-J., Kaviraj S., Deharveng J.-M., the GALEX Science Team 2005, ApJ, 619, L111